

Fluorescence enhancement of quantum emitters with different energy systems near a single spherical metal nanoparticle

Yingjie Zhang,¹ Ruoyang Zhang,¹ Qingru Wang,¹ Zhishuai Zhang,¹ Haibo Zhu,¹ Jiadong Liu,¹ Feng Song,^{1,*} Shanxin Lin,² and Edwin Yue Bun Pun²

¹*School of Physics, Nankai University, Tianjin 300071, P. R. China*

²*Department of Electronic Engineering, City University of Hong Kong, Tat Chee Avenue, Hong Kong, China*

**fsong@nankai.edu.cn*

Abstract: We present a theoretical study of the influence of a single spherical metal nanoparticle (MNP) on the fluorescence intensity of nearby emitters with two-level and multi-level energy systems. The enhancement factors of the excitation and relaxation processes are deduced. To reveal the interrelationship between the excitation and relaxation processes we adopt the rate equations of two-level fluorescent systems and upconversion fluorescent systems, and deduce the expression for the fluorescence enhancement factor. Our calculated results for the two-level systems agree well with reported experimental data. As to the upconversion fluorescent systems, our numerical results provide the first theoretical prediction showing that the MNP may selectively enhance a certain fluorescence process among various ones.

©2010 Optical Society of America

OCIS codes: (160.4236) Nanomaterials; (190.7220) Upconversion; (240.6680) Surface plasmons; (260.2510) Fluorescence.

References and links

1. E. M. Purcell, "Spontaneous emission probabilities at radio frequencies," *Phys. Rev.* **69**, 681 (1946).
2. P. Andrew, and W. L. Barnes, "Molecular fluorescence above metallic gratings," *Phys. Rev. B* **64**(12), 125405 (2001).
3. K. T. Shimizu, W. K. Woo, B. R. Fisher, H. J. Eisler, and M. G. Bawendi, "Surface-enhanced emission from single semiconductor nanocrystals," *Phys. Rev. Lett.* **89**(11), 117401 (2002).
4. J. Kalkman, C. Strohhofer, B. Gralak, and A. Polman, "Surface plasmon polariton modified emission of erbium in a metalodielectric grating," *Appl. Phys. Lett.* **83**(1), 30–32 (2003).
5. Y. Wang, and Z. P. Zhou, "Strong enhancement of erbium ion emission by a metallic double grating," *Appl. Phys. Lett.* **89**(25), 253122 (2006).
6. K. L. Shuford, M. A. Ratner, S. K. Gray, and G. C. Schatz, "Electric field enhancement and light transmission in cylindrical nanoholes," *J. Comput. Theor. Nanosci.* **4**, 239–246 (2007).
7. M. H. Chowdhury, K. Ray, S. K. Gray, J. Pond, and J. R. Lakowicz, "Aluminum nanoparticles as substrates for metal-enhanced fluorescence in the ultraviolet for the label-free detection of biomolecules," *Anal. Chem.* **81**(4), 1397–1403 (2009).
8. Y. Ito, K. Matsuda, and Y. Kanemitsu, "Mechanism of photoluminescence enhancement in single semiconductor nanocrystals on metal surfaces," *Phys. Rev. B* **75**(3), 033309 (2007).
9. C. Hagglund, M. Zach, and B. Kasemo, "Enhanced charge carrier generation in dye sensitized solar cells by nanoparticle plasmons," *Appl. Phys. Lett.* **92**(1), 013113 (2008).
10. M. Thomas, J.-J. Greffet, R. Carminati, and J. R. Arias-Gonzalez, "Single-molecule spontaneous emission close to absorbing nanostructures," *Appl. Phys. Lett.* **85**(17), 3863–3865 (2004).
11. S. Kühn, U. Håkanson, L. Rogobete, and V. Sandoghdar, "Enhancement of single-molecule fluorescence using a gold nanoparticle as an optical nanoantenna," *Phys. Rev. Lett.* **97**(1), 017402 (2006).
12. P. Bharadwaj, and L. Novotny, "Spectral dependence of single molecule fluorescence enhancement," *Opt. Express* **15**(21), 14266–14274 (2007).
13. P. Bharadwaj, P. Anger, and L. Novotny, "Nanoplasmonic enhancement of single-molecule fluorescence," *Nanotechnology* **18**(4), 044017 (2007).

14. R. Esteban, M. Laroche, and J.-J. Greffet, "Influence of metallic nanoparticles on upconversion processes," *J. Appl. Phys.* **105**(3), 033107 (2009).
15. T. Härtling, P. Reichenbach, and L. M. Eng, "Near-field coupling of a single fluorescent molecule and a spherical gold nanoparticle," *Opt. Express* **15**(20), 12806–12817 (2007).
16. M. Ringler, A. Schwemer, M. Wunderlich, A. Nichtl, K. Kürzinger, T. A. Klar, and J. Feldmann, "Shaping emission spectra of fluorescent molecules with single plasmonic nanoresonators," *Phys. Rev. Lett.* **100**(20), 203002 (2008).
17. P. Anger, P. Bharadwaj, and L. Novotny, "Enhancement and quenching of single-molecule fluorescence," *Phys. Rev. Lett.* **96**(11), 113002 (2006).
18. E. Verhagen, L. Kuipers, and A. Polman, "Enhanced nonlinear optical effects with a tapered plasmonic waveguide," *Nano Lett.* **7**(2), 334–337 (2007).
19. E. Verhagen, L. Kuipers, and A. Polman, "Field enhancement in metallic subwavelength aperture arrays probed by erbium upconversion luminescence," *Opt. Express* **17**(17), 14586–14598 (2009).
20. C. F. Bohren, and D. R. Huffman, *Absorption and Scattering of Light by Small Particles* (Wiley, New York, 1983).
21. M. Kerker, D.-S. Wang, and H. Chew, "Surface enhanced Raman scattering (SERS) by molecules adsorbed at spherical particles: errata," *Appl. Opt.* **19**(24), 4159 (1980).
22. Y.-L. Xu, "Electromagnetic scattering by an aggregate of spheres," *Appl. Opt.* **34**(21), 4573–4588 (1995).
23. R. Ruppin, "Decay of an excited molecule near a small metal sphere," *J. Chem. Phys.* **76**(4), 1681–1684 (1982).
24. X. M. Liu, X. F. Yang, F. Y. Lu, J. H. Ng, X. Q. Zhou, and C. Lu, "Stable and uniform dual-wavelength erbium-doped fiber laser based on fiber Bragg gratings and photonic crystal fiber," *Opt. Express* **13**(1), 142–147 (2005).
25. E. Desurvire, J. R. Simpson, and P. C. Becker, "High-gain erbium-doped traveling-wave fiber amplifier," *Opt. Lett.* **12**(11), 888–890 (1987).
26. P. B. Johnson, and R. W. Christy, "Optical Constants of the Noble Metals," *Phys. Rev. B* **6**(12), 4370–4379 (1972).
27. H. Lin, E. Y. B. Pun, S. Q. Man, and X. R. Liu, "Optical transitions and frequency upconversion of Er^{3+} ions in $\text{Na}_2\text{O-Ga}_3\text{Al}_2\text{Ge}_3\text{O}_{12}$ glasses," *J. Opt. Soc. Am. B* **18**(5), 602–609 (2001).

1. Introduction

The influence of the surrounding environment on the fluorescence process of quantum emitters has been studied extensively, starting off with Purcell [1]. Among various materials that affect fluorescence, metals are of great interest due to the plasmonic resonance of the free electrons with the excitation field. This plasmonic resonance, in turn, can couple strongly with the fluorescence process of nearby emitters. Theoretical and experimental studies of the influence of metallic nanostructures (surfaces, wires, particles, etc.) on fluorescence processes have been developed [2–17]. Nowadays, single molecule detection and spectroscopy are made possible as a result of the near-field optical techniques. In order to improve the detection efficiency, metal tips of various shapes are used to enhance the fluorescence intensity of single emitters [10–14]. According to currently developed theories, metal nanoparticles in the state of Localized Surface Plasmon Resonance (LSPR) can both enhance the excitation probability of the emitter and quench the fluorescent emission by absorbing energy from it [11–17]. Numerical calculations with experimental proof have been carried out to illustrate the interaction of a single metal nanoparticle with fluorescent emitters, which are approximated to be simple two-level systems [11–13], or three-level systems [14].

Currently there has been an increasing interest in probing electromagnetic local fields with erbium ions, in which the infrared fluorescence and upconversion fluorescence both exist [18,19]. The interaction of a metal nanoparticle with upconversion processes is discussed in a theoretical work [14], which has only explored one emission process of the upconversion fluorescent system. To the best of our knowledge, there has been no study of the real erbium ion system which involves the emission of photons with several ranges of frequencies.

In this paper, we present theoretical calculation of the interaction between a spherical metal nanoparticle (MNP) and the surrounding fluorescent emitter excited by external electromagnetic field. We treat the excitation and relaxation processes of the fluorescent emitter as dipole transitions, and regard the relaxation process as classical electric dipole radiation. With the aid of Mie theory [20], we can calculate the enhancement factor of the excitation probability which depends on the wavelength of the incident field. As to the relaxation processes, a series of expressions for the enhancement factors of various relaxation pathways can be deduced [21–23]. To reveal the mechanism of the enhancement of fluorescence

intensity, we adopt the steady state rate equations, which show the interrelationship of the excitation and relaxation processes, and provide expressions for the fluorescence enhancement factor. The calculated enhancement factor of fluorescence intensity for a two-level system is in well agreement with the reported experimental data, which shows the validity of the rate equation method and our calculation for various enhancement factors in the excitation and relaxation processes. Finally, we extend our calculation to the complex upconversion fluorescence process. After deriving the enhancement factor of the fluorescence intensity of erbium ions, we provide numerical results showing that the MNP with various sizes can either enhance or weaken the upconversion green fluorescence and the infrared fluorescence. The relative enhancement factor of the green light with respect to the infrared light is also calculated, and is shown to vary significantly with the MNP radius and the MNP-dipole distance. Therefore, we may enhance specific dipole transitions by changing these two factors. This result may be applied to tune erbium-doped lasers/fiber amplifiers [24,25] to emit/amplify light with a specific, single wavelength.

The paper is organized as follows. In section 2, the generalized theory of fluorescence enhancement near a single spherical metal nanoparticle is provided. In section 3, we deduce the enhancement factor of the fluorescence intensity for two-level systems and compare the result with the reported experimental data. In section 4, we calculate the enhancement factor of both the upconversion fluorescence and the infrared fluorescence of erbium ions, showing that LSPR may enhance either process. Section 5 is a summary of this article.

2. Generalized theory on the fluorescence enhancement

Generally, fluorescence consists of two kinds of processes, i.e., excitation and relaxation. Excitation denotes the transition from lower energy levels to higher levels by absorption of photons, while relaxation can occur both radiatively via the emission of photons and nonradiatively via various pathways. For the fluorescent emitter near the MNP, excitation is enhanced due to the enhancement of the local field. As to the relaxation process, radiative decay probability is affected and a new channel of nonradiative decay is introduced. The theory of the fluorescence enhancement is provided as follows.

2.1 Excitation

Suppose that an x -polarized plane wave is incident on a homogeneous, isotropic spherical metal particle with wave vector \mathbf{k} parallel to the z axis. A fluorescent emitter is located on the x axis with distance r' from the center of the sphere with radius a , as is shown in Fig. 1. The fluorescent emitter is excited by the local field which is the sum of the incident field and the field scattered by the sphere. As an approximation, we treat the excitation process as a dipole transition with dipole moment \mathbf{p} . According to Fermi's golden rule, the probability that the emitter is excited R is proportional to the square of the modulus of the perturbation Hamiltonian $|\mathbf{p} \cdot \mathbf{E}|^2$. Therefore, the enhancement factor of R is obtained as:

$$h_{ex}(\omega) = \frac{|\mathbf{p} \cdot \mathbf{E}(\mathbf{r}')|^2}{|\mathbf{p} \cdot \mathbf{E}_i(\mathbf{r}')|^2} \quad (1)$$

where ω is the angular frequency of the incident wave, \mathbf{E}_i is the incident electric field, and

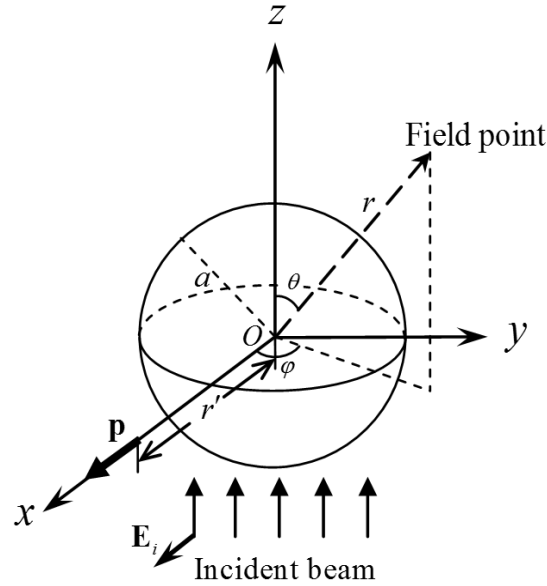


Fig. 1. Configuration of the theoretical model. The sphere represents the metal particle, and the dipole represents the fluorescent emitter.

$\mathbf{E}(\mathbf{r}')$ is the local field at the dipole point, which can be written as:

$$\mathbf{E}(\mathbf{r}') = \mathbf{E}_i(\mathbf{r}') + \mathbf{E}_s(\mathbf{r}'). \quad (2)$$

Here \mathbf{E}_s is the scattered field, the expression of which can be obtained from [20]. We assume that only the dipole oriented along the the x axis is excited [17], as is shown in Fig. 1. The enhancement factor can then be reduced to a simpler form:

$$h_{ex}(\omega) = \frac{|\mathbf{E}(\mathbf{r}')|^2}{|\mathbf{E}_i(\mathbf{r}')|^2} \quad (3)$$

2.2 Emission

In the calculation of the emission enhancement, we regard the excited fluorescent emitter as a classical electric dipole. In order to reveal the influence of the MNP on the relaxation process, we ignore the incident plane wave and regard the primary dipole field \mathbf{E}_{dip} as the field incident on the MNP. The magnetic permeabilities of the sphere and the surrounding medium are assumed to be equal to the magnetic permeability of the vacuum μ_0 . The angular frequency of the oscillating dipole ω' can be different from the angular frequency of the incident field ω , and may have one or several continuous range of values, depending on the fluorescence spectrum of the emitter. The incident dipole field and the scattered field can be obtained following the procedures provided in [21].

To show the influence of the MNP on the fluorescence properties of the emitter, we need to calculate the various related powers. That is, the far field radiated power of incident dipole field P_0 , the far field radiated power of the secondary scattered field P_{sc} , and the power absorbed by the MNP P_{abs} . General theories about the expression for these powers are provided in [22,23].

The total power for radiative decay, nonradiative decay, and energy transfer process of a fluorescent emitter is:

$$P_{total} = P_r + P_{nr0} + P_{abs}. \quad (4)$$

Here P_{nr0} is the intrinsic nonradiative decay power and is independent of the environment, thus it does not change because of the plasmonic oscillation inside the MNP.

These powers are related with the relaxation probabilities of the emitter. For the isolated dipole, the radiative decay probability can be obtained as:

$$\gamma_0 = \frac{P_0}{\hbar\omega'}. \quad (5)$$

The total decay probability and the nonradiative decay probability are obtained as:

$$\gamma_{total0} = \frac{\gamma_0}{\eta}, \quad (6)$$

$$\gamma_{nr0} = \frac{P_{nr0}}{\hbar\omega'} = \frac{1-\eta}{\eta} \gamma_0. \quad (7)$$

Here we have introduced η as the intrinsic quantum efficiency, defined as the fraction of emission probability to the total decay probability.

As to the dipole in the vicinity of the MNP, the radiative decay probability and total decay probability are modified due to the interaction of the dipole and the localized plasmonic oscillation inside the MNP:

$$\gamma_r = \frac{P_r}{\hbar\omega'}, \quad (8)$$

$$\gamma_{total} = \frac{P_{total}}{\hbar\omega'}. \quad (9)$$

The enhancement factor of the total decay probability is obtained as:

$$h_{decay} = \frac{\gamma_{total}}{\gamma_{total0}} = \eta \frac{P_{total}}{P_0}. \quad (10)$$

The presence of the MNP introduces energy transfer from the dipole to the MNP as a new channel to dissipate energy. The energy transfer probability is:

$$\gamma_{ET} = \frac{P_{abs}}{\hbar\omega'}. \quad (11)$$

The quantum efficiency of the dipole coupled to the MNP is obtained as follows:

$$\eta' = \frac{\gamma_r}{\gamma_{total}} = \frac{P_r}{P_{total}}. \quad (12)$$

The enhancement factor of the quantum efficiency is:

$$h_q = \frac{\eta'}{\eta} = \frac{1}{\eta} \frac{P_r}{P_{total}}. \quad (13)$$

Up till now, we have obtained the expressions for the excitation enhancement factor and the enhancement of the total decay probability, together with the enhancement of the quantum efficiency of the florescent emitter near the MNP. While the excitation enhancement depends on the wavelength of the incident plane wave, the modification of the various factors in the

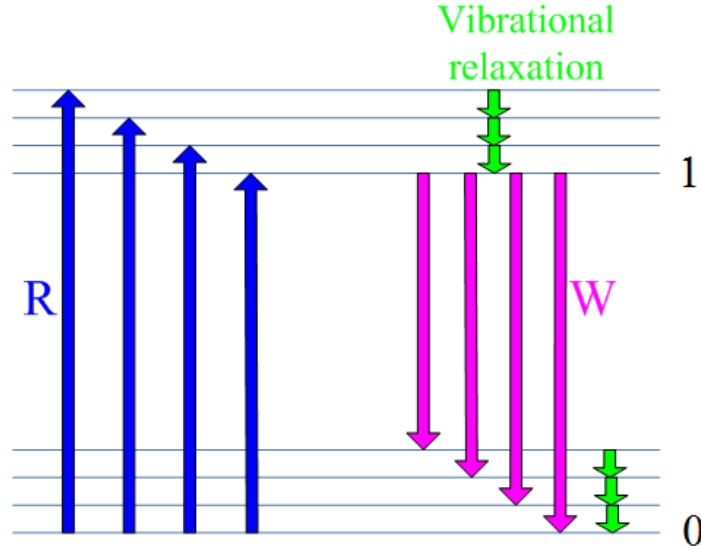


Fig. 2. Schematic diagram of a two-level system.

relaxation process does not rely on the excitation field, and is dependent on the emitted photon energy $\hbar\omega'$ (determined by the energy difference between the upper and lower transition levels) and the orientation of the dipole moment \mathbf{p} .

3. Enhanced fluorescence intensity of two-level systems

Currently, the enhancement of fluorescence intensity near metal nanoparticle(s) is generally viewed as the result of two independent processes: excitation enhancement and emission enhancement [11–13,15–17]. However, when taking into account the time evolution of the fluorescence process under continuous pumping, the excitation and relaxation processes of the fluorescent emitter should be interrelated. To show the relation of these two processes, we adopt the rate equations of the fluorescence process to deduce the expression for the fluorescence enhancement factor.

For two-level systems, the energy levels are shown in Fig. 2. Note that for each electronic level, there are many vibrational levels around it. In general, the relaxation processes between these vibrational levels are much faster than the transition between the two electronic levels. Therefore, it is reasonable to ignore these vibrational relaxation processes when writing the rate equations of the system. Thus, we can easily obtain the rate equations as follows:

$$\begin{aligned} \frac{dN_0}{dt} &= -N_0R + N_1W, \\ \frac{dN_1}{dt} &= N_0R - N_1W, \\ N_0 + N_1 &= N. \end{aligned} \quad (14)$$

where R and W are the excitation probability and total decay probability, respectively. And N is the total population of the fluorescent emitter, while N_0 and N_1 are the population of state $|0\rangle$ and state $|1\rangle$, separately. For a single emitter, $N=1$, and N_0 , N_1 denotes the probability that the emitter is at each energy level at the time t .

In the steady state, we can obtain the following results:

$$N_0 = \frac{NW}{W + R},$$

$$N_1 = \frac{NR}{W + R}.$$
(15)

The fluorescence rate is obtained as:

$$\Gamma_{fluor} = N_1 W \eta.$$
(16)

It should be noted that the fluorescence rate here means the number of photons emitted per unit time, and is different from the excitation and decay probability which is the probability of transition per unit time.

For weak excitation, the fluorescent emitter is in the thermal equilibrium state, thus satisfy the Boltzmann distribution law. Under this condition,

$$N_1 / N_0 = \exp\left(-\frac{E_1 - E_0}{k_B T}\right) = \exp\left(-\frac{\hbar\omega'}{k_B T}\right),$$
(17)

where E_1 and E_0 are the energy eigenvalues of the state $|1\rangle$ and $|0\rangle$, respectively. When the radiation wavelength is in the range of visible or infrared spectrum, we can get the relation:

$$N_1 \ll N_0.$$
(18)

Noting that $R/W = N_1/N_0$, we obtain:

$$R \ll W,$$
(19)

$$N_1 = \frac{NR}{W},$$
(20)

$$\Gamma_{fluor} = NR\eta.$$
(21)

Equation (21) shows that the fluorescence rate is proportional to the excitation probability and the quantum efficiency, which corresponds to the excitation and relaxation process, respectively. Thus, the enhancement factor of the fluorescence intensity is:

$$h_{fluor} = h_{ex} h_q.$$
(22)

This result is in agreement with those reported in [11–17]. To calculate this enhancement factor, we choose gold as the material for the metal nanoparticle, and the fluorescent emitter is taken to be Nile Blue, which has a simple two-level system. The dielectric constant of gold is obtained from [26], and various other parameters are taken from [12], which are listed as follows: $\eta = 1$, $\lambda = 637nm$, $n_0 = 1$, $a = 40nm$. The calculated results for the two-level system are shown in Fig. 3.

We can see that h_{ex} decreases rapidly with the decrease of dipole-MNP distance, while h_q rises until reaching unity. As to the fluorescence enhancement factor, it reaches maximum when the distance is $5nm$. Below this distance, the enhancement factor drops as a result of the quenching effect. It should be noted that classical electrodynamics will be invalid when the distance becomes too small (less than $2nm$), so will our calculated results. At larger distance, the fluorescence enhancement also decreases due to the decrease of excitation enhancement, and ultimately reaches unity, which means that the MNP will have no effect on the fluorescent dipole.

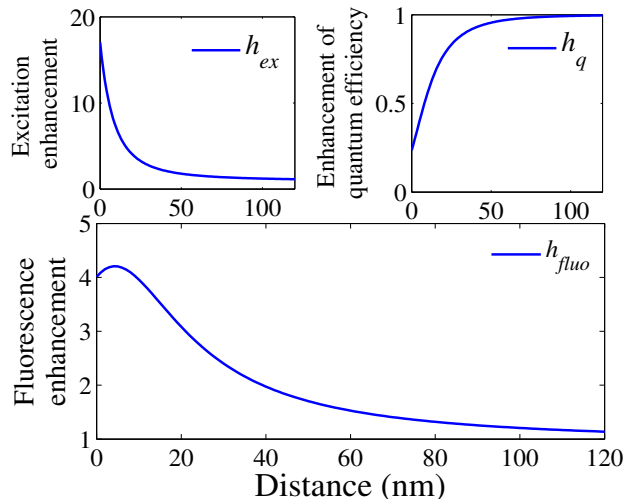


Fig. 3. (a) Excitation enhancement factor of the dipole in the vicinity of the MNP with a radius of 40nm. (b) Enhancement factor of quantum efficiency. (c) Fluorescence enhancement factor.

Taking into account the specific condition that the dielectric layer at the surface of the MNP increases the fluorescence enhancement by a factor 2-3 in the close vicinity of the MNP as reported in [12], our calculated results for the fluorescence enhancement are in well agreement with the experimental data in this reference.

4. Influence of MNP on nearby upconversion fluorescence systems

In this section, we focus on the simplification of multi-level fluorescence systems, and calculate the fluorescence enhancement factors of different fluorescence processes. The theory is outlined below with numerical results provided, showing the tunability of specific fluorescent transitions by using MNP.

4.1 Theory

To understand the fluorescence process of quantum emitters with complex energy levels, we can illustrate the interrelationship of the excitation and relaxation processes with the aid of the rate equations of the system. As an example, we have calculated the fluorescence intensity of green light (which generally dominates the visible spectrum) and infrared light for erbium ions. For simplicity, we only consider the excited state absorption (ESA) upconversion processes which results in green emission with the transition ${}^2H_{11/2} \rightarrow {}^4I_{15/2}$ and ${}^4S_{3/2} \rightarrow {}^4I_{15/2}$, together with the direct transition ${}^4I_{13/2} \rightarrow {}^4I_{15/2}$ which produces infrared light. Thus, we reduce the complex energy level diagram of erbium ions to a simple form, as shown in Fig. 4.

Similar to the treatment of the vibrational relaxation processes in two-level fluorescence systems, we assume that the MPR (Multi-phonon assisted Relaxation) processes $|2\rangle({}^4F_{7/2}) \rightarrow |2'\rangle({}^2H_{11/2})$, $|2\rangle \rightarrow |2''\rangle({}^4S_{3/2})$ and $|1\rangle({}^4I_{11/2}) \rightarrow |1'\rangle({}^4I_{13/2})$ (which is common in erbium doped crystals) are much faster than the excitation and emission processes. Therefore, we regard level $|1\rangle$ and level $|1'\rangle$ as one single level (level $|1\rangle$), and combine level $|2\rangle$, $|2'\rangle$, $|2''\rangle$ to two separate levels $|2'\rangle$ and $|2''\rangle$ (i.e. “move” the population of level $|2\rangle$ to

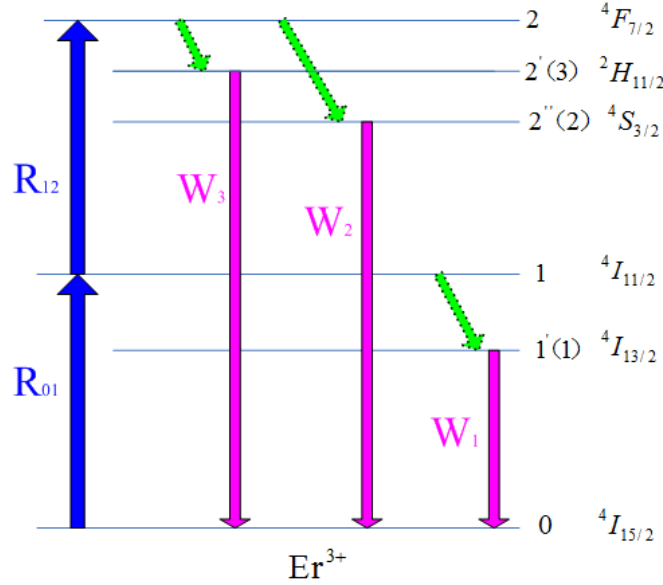


Fig. 4. Schematic diagram of energy levels for erbium ions.

$|2'\rangle$ and $|2''\rangle$). For simplicity, we write level $|2''\rangle$ and $|2'\rangle$ as level $|2\rangle$ and $|3\rangle$ in the following calculation. We further assume that the branching ratio from higher excited states $|2\rangle$ and $|3\rangle$ to the ground state $|0\rangle$ (${}^4I_{15/2}$) equals to 1, and the rate equations can be written as follows:

$$\begin{aligned}
 \frac{dN_0}{dt} &= -R_{01}N_0 + W_1N_1 + W_2N_2 + W_3N_3, \\
 \frac{dN_1}{dt} &= R_{01}N_0 - (W_1 + R_{12})N_1, \\
 \frac{dN_2}{dt} &= \alpha_2 R_{12}N_1 - W_2N_2, \\
 \frac{dN_3}{dt} &= \alpha_3 R_{12}N_1 - W_3N_3, \\
 N_0 + N_1 + N_2 + N_3 &= N,
 \end{aligned} \tag{23}$$

where we have introduced α_2 and α_3 ($\alpha_2 + \alpha_3 = 1$) as the probabilities that the erbium ion at state ${}^4F_{7/2}$ relaxes to state ${}^4S_{3/2}$ and state ${}^2H_{11/2}$, respectively. N_i is the population of level $|i\rangle$ ($i = 0, 1, 2, 3$), and N is the total population of erbium ions. At steady state we can obtain the following results:

$$\begin{aligned}
N_1 &= \frac{N}{\frac{W_1 + R_{12}}{R_{01}} + 1 + \alpha_2 \frac{R_{12}}{W_2} + \alpha_3 \frac{R_{12}}{W_3}}, \\
N_2 &= \alpha_2 \frac{R_{12}}{W_2} N_1, \\
N_3 &= \alpha_3 \frac{R_{12}}{W_3} N_1.
\end{aligned} \tag{24}$$

The fluorescence rate of the transition $|i\rangle \rightarrow |0\rangle$ ($i = 0, 1, 2, 3$) can be written as:

$$\Gamma_{fluoi} = N_i W_i \eta_i, \tag{25}$$

where η_i is the intrinsic quantum efficiency of the transition $|i\rangle \rightarrow |0\rangle$. We can see that the fluorescence rate of every level depends on all the parameters R and W . To calculate the enhancement factor of the fluorescence rate, we need to know the parameters R and W for the isolated emitter, together with the enhancement factor for each R and W for the emitter in the vicinity of the MNP.

However, the results can be much simpler when we calculate the relative enhancement factor of the green light compared to the infrared light. In fact, the ratio of the fluorescence intensity of the transition $|i\rangle \rightarrow |0\rangle$ ($i = 2, 3$) with respect to that of $|1\rangle \rightarrow |0\rangle$ can easily be obtained by using Eq. (25) as:

$$\frac{\Gamma_{fluoi}}{\Gamma_{fluo1}} = \frac{N_i W_i \eta_i}{N_1 W_1 \eta_1}. \tag{26}$$

According to Eq. (24), $N_i/N_1 = \alpha_i R_{12}/W_i$. Therefore,

$$\frac{\Gamma_{fluoi}}{\Gamma_{fluo1}} = \alpha_i \frac{R_{12} \eta_i}{W_i \eta_1}. \tag{27}$$

Assume that α_i do not change because of the presence of the MNP, we get the relative enhancement factor:

$$\frac{h_{fluoi}}{h_{fluo1}} = \frac{h_{ex} h_{qi}}{h_{decay1} h_{q1}}. \tag{28}$$

where h_{fluoi} , h_{qi} and h_{fluo1} , h_{q1} are the enhancement of fluorescence rate and quantum efficiency for the dipole transition $|i\rangle \rightarrow |0\rangle$ and $|1\rangle \rightarrow |0\rangle$, respectively. h_{decay1} is the enhancement of total decay probability for the transition $|1\rangle \rightarrow |0\rangle$.

In order to understand the basic enhancement mechanisms of the upconversion process in the vicinity of the MNP, we would like to reduce Eqs. (24-25) to simpler forms. To reach this goal, we need to restrict the excitation condition to the weak excitation, where the erbium ions are in the thermal equilibrium state. Hence, similar to Eq. (17), we have:

$$\begin{aligned}
N_i/N_1 &= \exp\left(-\frac{E_i - E_1}{k_B T}\right), \\
N_i/N_1 \cdot W_i/W_1 &= W_i/W_1 \exp\left(-\frac{E_i - E_1}{k_B T}\right).
\end{aligned} \tag{29}$$

where E_i ($i = 2, 3$) and E_1 are the energy eigenvalues of the state $|i\rangle$ and $|1\rangle$, respectively. Normally, for erbium ions, we can obtain the following relations:

$$\begin{aligned} N_i/N_1 &\ll 1, \\ N_i/N_1 \cdot W_i/W_1 &\ll 1. \end{aligned} \quad (30)$$

Noting that $N_i/N_1 = \alpha_i R_{12}/W_i$, we get the relations:

$$\begin{aligned} R_{12}/W_i &\ll 1, \\ R_{12}/W_1 &\ll 1. \end{aligned} \quad (31)$$

Since the excitation wavelength for the transition ${}^4I_{15/2} \rightarrow {}^4I_{11/2}$ and ${}^4I_{11/2} \rightarrow {}^4F_{7/2}$ are the same, we can write:

$$R_{01} \approx R_{12}. \quad (32)$$

Thus, Eq. (24) is reduced to:

$$\begin{aligned} N_1 &= \frac{NR_{01}}{W_1}, \\ N_i &= \alpha_i \frac{NR_{01}R_{12}}{W_1W_i}, (i=2,3) \end{aligned} \quad (33)$$

Substituting Eq. (33) into Eq. (25), we obtain:

$$\begin{aligned} \Gamma_{flu01} &= NR_{01}\eta_1, \\ \Gamma_{fluoi} &= \alpha_i NR_{01}R_{12}\eta_i/W_1. \end{aligned} \quad (34)$$

So far, we have made several assumptions about the excitation condition and the fluorescent transition processes. Nevertheless, the results expressed by Eq. (34) are quite reasonable. The expression for Γ_{flu01} denotes that the enhancement factor is equal to the product of the excitation enhancement and the enhancement of quantum efficiency, which is in good agreement with that of the two-level fluorescent system. In fact, since $R_{12} \ll W_1$, the fluorescent transition occurs mainly between the states $|0\rangle$ and $|1\rangle$. Therefore, the infrared fluorescence process can be approximated to be two-level transitions. As for the expression of Γ_{fluoi} , it also includes the two-step excitation probability $R_{01}R_{12}$ and the quantum efficiency of the emission process η_i . Besides, there's one more item $\tau_1 = 1/W_1$, which is the lifetime of the metastable energy level $|1\rangle$. This is due to the fact that the population of level $|1\rangle$ is proportional to its lifetime and that the transition rate from level $|1\rangle$ to level $|i\rangle$ is proportional to the population of level $|1\rangle$. Thus, we can easily obtain the relation $\Gamma_{fluoi} \propto \tau_1$.

The enhancement factor of each emission rate is obtained as:

$$\begin{aligned} h_{flu01} &= h_{ex}h_{q1}, \\ h_{fluoi} &= \frac{h_{ex}^2h_{qi}}{h_{decay1}}. \end{aligned} \quad (35)$$

Using Eqs. (3) (10) (13) (28) (35), we are able to calculate the exact value of h_{fluoi}/h_{flu01} , and the value of h_{flu01} and h_{fluoi} in the weak excitation regime.

4.2 Numerical results

We have calculated the enhancement of the 547nm upconversion fluorescence ($|2\rangle \rightarrow |0\rangle$), the enhancement of the 1533nm infrared fluorescence ($|1\rangle \rightarrow |0\rangle$), and their relative enhancement for erbium ions near the MNP with three different values of radius: 50nm, 100nm, 150nm. The quantum efficiencies of erbium ions in absence of the MNP and the refractive index of the medium used in our calculation are taken from [27]. Specifically, the quantum efficiencies of the 547nm upconversion fluorescence and the 1533nm infrared fluorescence are taken to be 0.0085 and 1, respectively. The excitation wavelength is 973nm, and the refractive index of the medium ($\text{Na}_2\text{O} \cdot \text{Ca}_3\text{Al}_2\text{Ge}_3\text{O}_{12}$ glass) is calculated using the equation $n_0 = A + B/\lambda^2$, where $A = 1.6013$, $B = 8457\text{nm}^2$. The calculated results are shown in Fig. 5.

It can be seen that both the infrared fluorescence and the upconversion fluorescence are enhanced when the MNP radius is 50nm. As to the case when the MNP radius is 100nm or

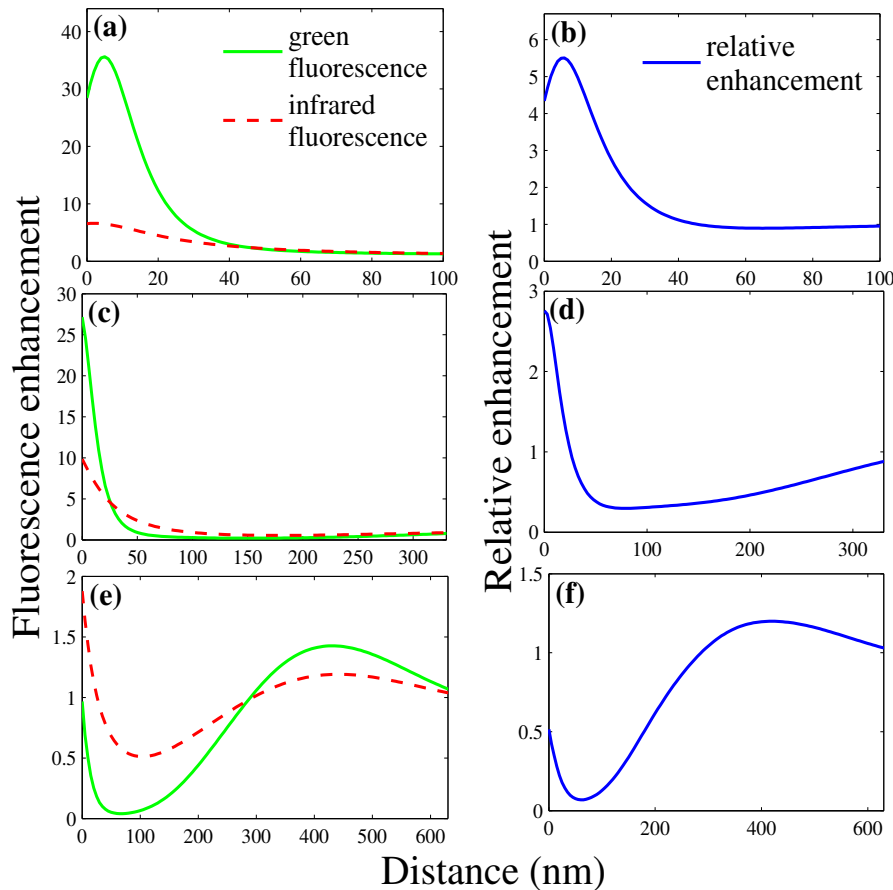


Fig. 5. The red dashed curve and the green solid curve in (a) (c) (e) denote the infrared and green fluorescence enhancement factors of erbium ions in the vicinity of MNP with radius 50nm, 100nm and 150nm, respectively. The blue solid curve in (b) (d) (f) is the relative enhancement of the 537nm upconversion fluorescence with respect to the 1533nm infrared fluorescence of erbium ions near MNP with radius 50nm, 100nm and 150nm, separately.

150nm, both processes may either be enhanced or weakened with the change of the MNP-dipole distance. For the relative enhancement factor, it is greater than 1 when the MNP radius is 50nm, revealing that the MNP favors the upconversion process. When the MNP becomes larger, this

factor drops. For MNP with radius 100nm , this factor is greater than 1 when the dipole-MNP distance is smaller than 26nm , and falls under 1 as the distance becomes larger. As to the 150nm radius MNP, the fluorescence enhancement of the infrared emission is larger than that of the upconversion fluorescence when the dipole-MNP distance is smaller than 287nm .

These numerical results show that the MNP may either enhance or weaken the infrared fluorescence and the upconversion fluorescence of the nearby erbium ions. By tuning the MNP radius and the dipole-MNP distance, we can selectively enhance either fluorescence process.

5. Conclusion

In conclusion, we have studied and provided insights into the effect of a metal nanoparticle on the fluorescence process of nearby emitters. Specifically, we have calculated the fluorescence enhancement factor of quantum emitters with two-level and multi-level energy systems near a single spherical metal nanoparticle. Our results show that the presence of MNP makes it possible to selectively enhance either the upconversion fluorescence or the infrared fluorescence of erbium ions.

Acknowledgments

This work was supported by NSFC 90923035, 973 Program 2006CB302904, NSFC J0730315, and the “100 Projects” of Creative Research for Undergraduates of Nankai University under project No. BX6-293.